Polymer Chemistry

Accepted Manuscript

This is an *Accepted Manuscript*, which has been through the Royal Society of Chemistry peer review process and has been accepted for publication.

Accepted Manuscripts are published online shortly after acceptance, before technical editing, formatting and proof reading. Using this free service, authors can make their results available to the community, in citable form, before we publish the edited article. We will replace this *Accepted Manuscript* with the edited and formatted *Advance Article* as soon as it is available.

You can find more information about *Accepted Manuscripts* in the Information for Authors.

Please note that technical editing may introduce minor changes to the text and/or graphics, which may alter content. The journal's standard Terms & Conditions and the Ethical guidelines still apply. In no event shall the Royal Society of Chemistry be held responsible for any errors or omissions in this *Accepted Manuscript* or any consequences arising from the use of any information it contains.

ROYAL SOCIETY OF CHEMISTRY

www.rsc.org/polymers

Development of Polycarbonate-containing Block Copolymers for Thin Film Self-assembly Applications

Ankit Vora*, Rudy J. Wojtecki, Kristin Schmidt, Anindarupa Chunder, Joy Y. Cheng, Alshakim Nelson and Daniel P. Sanders

IBM Research – Almaden, 650 Harry Rd., San Jose, California 95120

KEYWORDS. PS-*b*-PTMC, Poly(trimethylene carbonate), BCP fractionation, contrast enhanced DOSY, thin film self-assembly, DSA

Abstract

Access to well-defined materials is one of the key requirements for successful implementation of block copolymer-based lithography for advanced semiconductor nodes. We report on the development of polystyrene-*b*-polytrimethylene carbonate (PS-*b*-PTMC) block copolymer (BCP) using organocatalytic ring opening polymerization of trimethylene carbonate (TMC) from hydroxyl-functional polystyrene macroinitiator as a materials candidate for directed self-assembly applications. The impact of organocatalyst choice and the extent of TMC conversion on the quality of PS-*b*-PTMC BCP was studied using gel permeation chromatography and nuclear magnetic resonance (NMR) spectroscopy techniques. As a direct method to identify PTMC homopolymer content in the resulting BCPs, a new NMR-based technique was developed. Finally, the influence of BCP purity on the thin film morphology was studied using atomic force microscopy and grazing incidence small angle x-ray scattering techniques. Our

results indicate that the PTMC homopolymer impurity negatively impacts the thin film morphology, which is extremely important for potential lithographic applications.

INTRODUCTION

Block copolymers (BCPs), comprised of two or more covalently bonded incompatible blocks, can microphase separate into a rich variety of ordered morphologies ranging from spheres, cylinders, lamellae and more complex structures from 5-100 nm length scales.[1–3] As a result, block copolymers have gained considerable attention for a diverse range of applications, such as in surfactants, pigment dispersants, organic photovoltaics, nanomedicine, nanoporous

membranes, photonic crystals, air-gaps for dielectrics, high density storage media and next generation lithography.[4–14]

The ability to manufacture smaller, faster and more efficient microelectronic components governs the rate of advancement in semiconductor industry and presents one of the major technological challenges. There is a pressing need to develop scalable solutions for next generation lithography to obtain smaller well-defined features and patterns. Directed self-assembly (DSA) of block copolymers has emerged as a promising candidate to provide a materials-based resolution enhancement technique to extend 193 immersion and/or extreme UV (EUV) lithography to provide sub-lithographic feature sizes.

Poly(styrene-*b*-methylmethacrylate) (PS-*b*-PMMA) is one of the most extensively studied material for DSA using various graphoepitaxy[15] and chemoepitaxy[11] schemes because of its ready availability and simple processing conditions.[16–19] While PS-*b*-PMMA is the leading candidate as a first generation DSA material, the minimum feature size is limited to about 10 nm half-pitch (hp) due to the relatively weak segregation strength between the PS and the PMMA blocks, defined by the Flory-Huggins interaction parameter, χ. The χ also influences the interfacial width between the two domains impacting the line-edge roughness. In addition, due to the limited dry-etch selectivity between the PS and the PMMA blocks, the ability to selectively remove the PMMA domain is difficult at smaller feature sizes. These shortcomings of PS-*b*-PMMA were recently demonstrated by Wan and colleagues who showed that even though it was possible to obtain a full pitch of 18.5 nm with PS-*b*-PMMA, successful removal of the PMMA domains and subsequent pattern transfer was only feasible till 22 nm full pitch features.[20] To overcome these limitations of PS-*b*-PMMA, several groups have reported BCPs

with higher χ parameter and enhanced etch selectivity between the two blocks to enable sub-20 nm full pitch patterning.[21–32]

We decided to develop aliphatic polycarbonate (PC) high χ BCPs as a potential platform for DSA-enabled future semiconductor nodes. PC-based BCPs offer several advantages as a wide range of functional cyclic carbonate monomers can be readily synthesized allowing easy tuning of the χ parameter by changing the chemical composition of the polycarbonate block. Additionally, polycarbonates can be wet and dry etched, significantly enhancing the etch selectivity between the blocks to cleanly remove the polycarbonate block for subsequent pattern transfer. These properties of polycarbonates offer a very flexible platform for thin film self-assembly applications.

Recent developments in the field of organocatalysis have enabled controlled ROP of strained cyclic monomers such as aliphatic carbonates and lactones.[33,34] This robust synthetic strategy offers access to a variety polymeric architectures such as block[35,36], graft[37], stars[38] and dendrimers[39] with precise molecular weight control, in-chain functionality and narrow polydispersities.[40] The synthetic diversity and tailorable polymer characteristics have made this an attractive approach for a variety of applications including biomaterials,[41,42] drug delivery,[43] wound healing,[44] antimicrobials[45,46] and nanoimprint lithography,[47] to name a few.

Herein, we report the development of a polystyrene-*b*-polycarbonate (PS-*b*-PTMC) block copolymer (Scheme 1) platform as a candidate for high-χ material for thin film self-assembly applications. While many functional cyclic carbonate monomers are available for ROP from hydroxyl-functional polystyrene (PS-OH) macroinitiator, initial studies were done using

trimethylene carbonate (TMC) as a model carbonate monomer. TMC is the simplest carbonate monomer without any ester or ether side groups making it easier to study effects of the reaction conditions on the BCP quality. Specifically, in this work, effect of organocatalyst (base v/s acid) and TMC monomer conversion were studied. A novel BCP fractionation solvent mixture was used to obtain clean PS-*b*-PTMC BCPs by removing PTMC homopolymer formed as a side-reaction during the ROP polymerization of TMC. In addition, we report a new NMR-based technique, contrast enhanced diffusion ordered spectroscopy (CEDOSY) to study the purity of the polycarbonate-containing BCPs. Finally, the thin film morphologies of the non-purified and the purified BCPs were investigated using atomic force microscopy (AFM) and grazing incidence small angle x-ray scatterning (GISAXS) to determine the impact of PTMC homopolymer on self-assembly performance.

Scheme 1. Synthesis of PS-*b*-PTMC BCP using DBU or DPP Organocatalyst

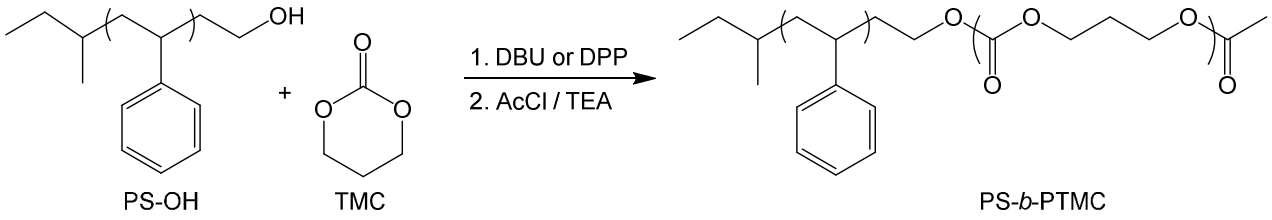

Experimental Section

Materials. All chemicals were received from Sigma-Aldrich Corporation and used as received unless specified otherwise. Diphenyl phosphate (DPP) was dried by azeotropic distillation from toluene to remove any water and stored in a nitrogen dry box. 1,8-diazabicyclo[5.4.0]undec-7-ene (DBU) was dried and distilled over CaH_2 and stored in a nitrogen dry box in a vial as a 10 wt% solution in anhydrous toluene. Trimethylene carbonate (TMC) was received from Richman Chemical Co. TMC was recrystallized three times from dry toluene and dried over high vacuum for 48 hours to remove any trace quantities of toluene. The resulting monomer was stored in a desiccator until it was used for polymerization. AZEMBLY™ NLD-303, a poly(methyl methacrylate) (PMMA) brush polymer solution in propylene glycol monomethyl ether acetate (PGMEA), and hydroxyl-functional polystyrene (PS-OH, M_n = 6600 g/mol, PDI = 1.04) macroinitiator were provided by EMD Performance Materials Corporation and were used as received.

Methods. ^{1}H NMR spectra were acquired in $CDCl_3$ using a Bruker Avance 400 MHz spectrometer 400-MHz; chemical shifts (δ) are expressed in parts per million (ppm) relative to TMS.

Gel permeation chromatography was performed using a Waters Advanced Polymer Chromatograph equipped with three ACQUITY APC™ XT columns (4.6 mm × 150 mm) connected in series with increasing pore size (45, 125 and 200 Å), using THF as the eluant, and calibrated with polystyrene standards (750 – 10^6 g/mol).

Atomic force microscopy (AFM) measurements were done using a Digital Instruments 3100 AFM with a 1 N/m spring constant silicon nitride cantilever operated in a tapping mode. Scan size and speed were set at 2 µm x 2 µm area and 1 Hz, respectively. Power spectral density

(PSD) data used to determine the periodical spacing between BCP domains was processed by the Digital Instruments software, Nanoscope version 5.30.

Grazing incidence small angle x-ray scattering (GISAXS) was collected at the Advanced Light Source (ALS) at Lawrence Berkeley National Laboratory (LBNL) at beam line 7.3.3.[48] The incident x-ray energy was 10 keV and the sample to detector distance was 4 m. Scattered x-rays were collected using a Pilatus 2M detector. Data was normalized for incoming x-ray intensity, film thickness and wafer size, averaged, and integrated along q_x = 0.028 $Å^{-1}$ using the IRENA package, developed by I. Ilavsky.[49] The scattering profiles were analyzed by fitting a series of Voigt peaks and an exponential background to the 1D data. The periodicity was calculated from the 1st order Bragg peak by $d = 2\pi/q$.

CEDOSY Sample Preparation and Evaluation. All CEDOSY samples utilized 10 mg of polymer that was first dissolved in 0.8 ml of $CDCl_3$ followed by the addition of 1.0 ml of CD_3OD until reaching the cloud point of the polymer solution. Solutions were then immediately transferred into 5 mm NMR tubes and directly analyzed. CEDOSY measurements were performed on Bruker Avance 300 MHz equipped with a VSP 300 probe at a constant temperature of 292.2 K. The ^1H chemical shifts were referenced to residual $CHCl_3$ signals. DOSY spectra were obtained using a stimulated echo pulse sequence with bipolar gradients (STEBPGP). 64 scans were collected at each increment with a total of 32 increments taken. Raw DOSY-NMR data was processed in MestReNova version 8.1.2-11880 using the model function data analysis options. Before fitting the array of spectra phase correction was performed followed by a baseline correction utilizing a Bernstein polynomial fit (polynomial order 3). Exponential and Gaussian apodization functions

were used during data processing with a line broadening factor of 1.0 Hz. The peak intensities were normalized for comparison between samples.

Representative Base Catalyzed Polymerization of TMC from PS-OH Macroinitiator. To an oven dried 4 ml glass vial equipped with a magnetic stir bar, PS-OH (0.15 g, 0.0227 mmol, M_n = 6600 g/mol, PDI = 1.04), TMC (0.192 g, 1.88 mmol) and anhydrous dichloromethane (DCM)(1.90 ml) were added. The reaction mixture was stirred until the PS-OH macroinitiator and TMC were completely dissolved in DCM, upon which DBU (17.5 mg, 0.113 mmol, 5 eq. w.r.t. PS-OH) was added. The reaction mixture was stirred at room temperature for 24 hours in a glove box. The reaction vial was removed from the glove box and the reaction was stopped by adding DCM (1 ml), TEA (0.1 ml, 1.35 mmol) and acetyl chloride (0.25 ml, 3.52 mmol). The reaction was further stirred for two hours at room temperature. The resulting polymer was isolated by precipitating the reaction mixture in methanol. The product was collected in a frit funnel by removing methanol under vacuum and the resulting solids were redissolved in THF to form a 20 wt% solution and reprecipitated in methanol. The solid was collected in a frit funnel and dried under vacuum at 40 °C for two hours to obtain the resulting compound. M_{nGPC} = 14,100 g/mol, PDI = 1.08; M_{nNMR}: polystyrene (PS) block, DP = 63, M_n = 6600 g/mol, poly(trimethylene carbonate) (PTMC) block, DP = 74, M_n = 7600 g/mol. TMC % conversion (^{1}H NMR) ~ 90%. Volume fraction of PTMC block, Vf_{PTMC} ~ 0.47. δ_{PS} = 1.02 g/cm^3 and δ_{PTMC} = 1.30 g/cm^3 (Figure S1).[50]

Representative Acid Catalyzed Polymerization of TMC from PS-OH Macroinitiator. To an oven dried 4 ml glass vial equipped with a magnetic stir bar, PS-OH (0.15 g, 0.0227 mmol, Mn = 6600 g/mol, PDI = 1.04), TMC (0.192 g, 1.88 mmol) and DCM (1.90 ml) were added. The reaction

mixture was stirred until the PS-OH macroinitiator and TMC were completely dissolved in DCM, upon which DPP (28 mg, 0.113 mmol, 5 eq. w.r.t. PS-OH) was added. The reaction mixture was stirred at room temperature for 58 hours in a glove box. The reaction vial was removed from the glove box and the reaction was stopped by adding DCM (1 ml), TEA (0.1 ml, 1.35 mmol) and acetyl chloride (0.25 ml, 3.52 mmol). The reaction was further stirred for two hours at room temperature. The resulting polymer was isolated by precipitating the reaction mixture in methanol. The product was collected in a frit funnel by removing methanol under vacuum and the resulting solids were redissolved in THF to form a 20 wt% solution and reprecipitated in methanol. The solid was collected in a frit funnel and dried under vacuum at 40 °C for two hours to obtain the resulting compound, M_{nGPC} = 21,500 g/mol PDI = 1.02; Mn_{NMR}: polystyrene (PS) block M_n = 6600 g/mol, poly(trimethylene carbonate) (PTMC) block Mn = 7500 g/mol. TMC % conversion (^{1}H NMR) ~ 88%. Volume fraction of PTMC block, Vf_{PTMC} ~ 0.47.

Representative Fractionation of PS-*b*-PTMC BCP in Methanol:acetonitrile Solvent Mixture. 100 mg of PS-b-PTMC BCP synthesized with DBU catalyst described above was dissolved in THF to form a 20 wt% solution and the polymer was precipitated in methanol:acetonitrile (20 ml, 60:40 v/v). The precipitated solids and the solvents were collected in a 30 ml glass vial and the solids were collected by centrifuging at 4000 rpm at 0° C followed by decanting the solvent and drying the solids in a vacuum oven at 40° C for two hours to obtain the purified BCP. Mn_{GPC} = 14,400 g/mol, PDI = 1.05; Mn_{NMR}: polystyrene (PS) block Mn = 6600 g/mol, poly(trimethylene carbonate) (PTMC) block Mn = 4800 g/mol. Volume fraction of PTMC block, Vf_{PTMC} ~ 0.36.

Representative Thin Film Preparation and Self-assembly of PS-*b*-PTMC BCP. AZEMBLY™ NLD-303, a poly(methyl methacrylate) (PMMA) brush polymer solution in PGMEA, was spin coated at 2000 rpm on a silicon wafer. The coated wafer was baked at 250 °C for 2 minutes on a hot plate and immediately cooled to room temperature. The resulting substrate was treated with a solvent (PGMEA) rinse step to remove any non-grafted PMMA brush polymer. Next, a 1.2 wt% solution of PS-*b*-PTMC BCP was prepared by dissolving the BCP in PGMEA and filtering using a 0.2 µm PTFE filter. The BCP solution was spin coated onto the PMMA underlayer (UL) modified silicon wafer obtained as described above. The BCP was annealed at 140 °C for 5 minutes and cooled to room temperature to enable phase-separation. The thin film morphology was characterized by AFM and GISAXS.

Results and Discussion

Effect of Organocatalyst on Ring Opening Polymerization of Trimethylene Carbonate using PS-OH Macroinitiator. In our quest to make polycarbonate-containing block copolymers for sub-20 nm pitch patterning application, both basic and acidic organic catalysts were evaluated for ring opening polymerization (ROP) of trimethylene carbonate (TMC) using hydroxyl-functional polystyrene (PS-OH) macroinitiator (Scheme 1). All reactions were done in an oven dried glassware in a nitrogen dry box at room temperature in dichloromethane (DCM) (1 M carbonate monomer). 1,8-diazabicyclo[5.4.0]undec-7-ene (DBU) or diphenyl phosphate (DPP) (5 M PS-OH) were used as the basic or acidic organic catalysts, respectively, as previously reported by other groups.[51–53] The reactions were quenched and the hydroxyl end-group on the polymer chain was capped in-situ by adding acetyl chloride and triethylamine followed by allowing the

mixture to stir for at least 30 min at room temperature. Finally, the polymers were isolated by precipitating twice in methanol.

Table 1. Synthesis and Purification of PS-*b*-PTMC BCPs

				Before Fractionation				After Fractionation			
Run #	Catalyst type	% Conv. of carbonate monomer[a]	Reaction time (hours)	Mn_{GPC} g/mol	PDI	Mn_{NMR}[b] g/mol	Vf_{PTMC}	Mn_{GPC} g/mol	PDI	Mn_{NMR}[b] g/mol	Vf_{PTMC}
1	DBU	90	24	14100	1.08	6.6k-*b*-7.6k	0.47	14400	1.05	6.6k-*b*-4.8k	0.36
2	DPP	88	57.5	21500	1.02	6.6k-*b*-7.5k	0.47	21000	1.02	6.6k-*b*-7.0k	0.45
3	DBU	50	9	11700	1.06	6.6k-*b*-4.3k	0.34	12500	1.03	6.6k-b-2.4k	0.23
4	DPP	50	24	15200	1.02	6.6k-*b*-4.4k	0.34	16400	1.02	6.6k-*b*-3.6k	0.31

[a] Analyzed by ^{1}H NMR. [b] Molecular weight of PS-*b*-PTMC as measured by ^{1}H NMR.

An initial experiment to study the chain extension of PS-OH was done by ROP of TMC using the base catalyst DBU (Table 1, Example 1).[51] The GPC trace of this polymer showed a trimodal molecular weight distribution with a high molecular weight shoulder, a low molecular tail and a PDI of 1.08 (Figure 1a). It has been previously reported that at higher conversions of the cyclic carbonyl monomers when superbases like TBD and DBU are used as catalysts, the resulting polymers show significant broadening of the molecular weight distributions resulting in bimodal GPC traces with a high molecular weight shoulder.[54–56]

To study the effect of monomer conversion on the BCP quality, a PS-*b*-PTMC BCP with around 50% conversion of the TMC monomer was synthesized (Table 1, Example 3) using the same catalyst. Unlike the BCP formed by 90% conversion of the TMC monomer, the GPC trace (Figure S2) of the BPC made by 50% conversion of the TMC monomer did not show any appreciable high molecular weight shoulder and had a PDI of 1.06. This result indicates that by limiting the monomer conversion, the intermolecular and coupling side reactions can be

reduced for the DBU catalyzed polymerization reactions. In addition, it was noticed that the low molecular weight tail was also significantly reduced indicating smaller amount of impurity in the BCP.

Alternatively, diphenyl phosphate (DPP) was used as an organic-acid to synthesize PS-*b*-PTMC BCPs (Table 1, Examples 2 & 4). Unlike the DBU catalyzed BCPs, the GPC traces for the DPP catalyzed BCPs did showed only a very small high molecular weight shoulder (< 3%) for both 90 % (Figure 1b) and 50 % conversion of TMC (Figure S3), confirming that for the DPP catalyzed ROP of TMC coupling side reactions were minimal. In addition, the GPC trace did not show any noticeable low molecular weight shoulder which indicated that the resulting diblock copolymers were relatively pure with a only small amount of side products.

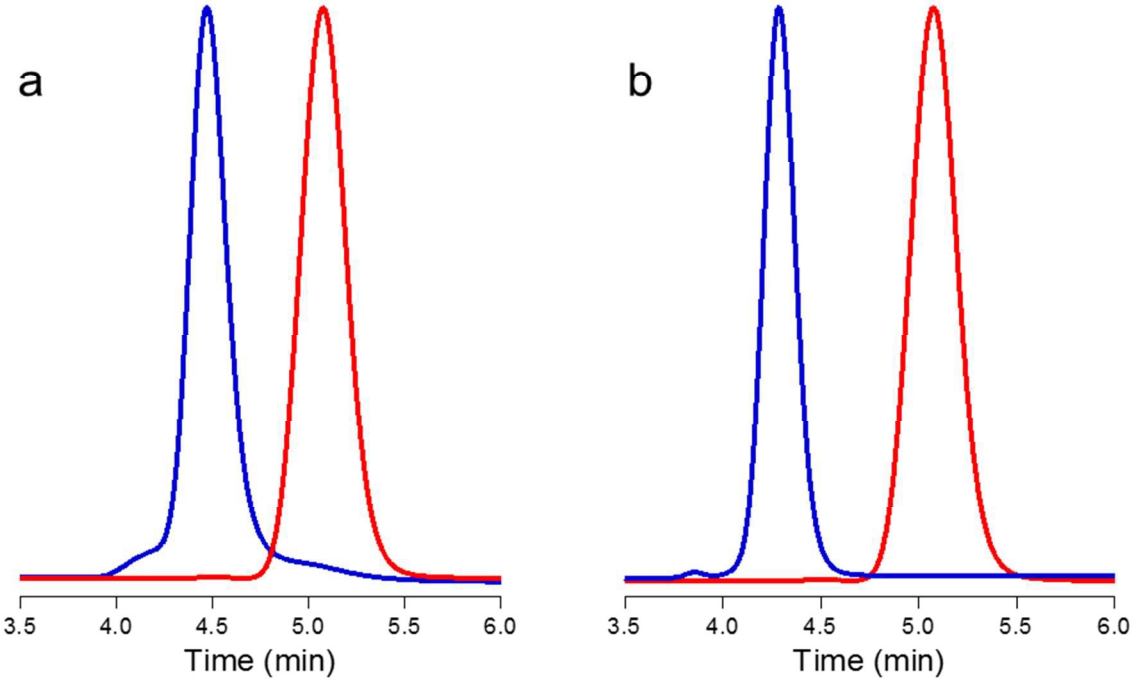

Figure 1. GPC traces for PS-OH (red), M_n = 6600 g/mol, PDI = 1.04 and PS-*b*-PTMC (blue) BCP using (a) DBU catalyst, M_n = 14,100 g/mol, PDI = 1.08 (Table 1, Example 1, before fractionation)

and (b) DPP Catalyst, M_n = 21,500 g/mol, PDI = 1.02 (Table 1, Example 2, before fractionation). The reactions were terminated at 90 and 88% conversion of TMC monomer, respectively.

Fractionation of Block Copolymers. The morphology, domain spacing and domain-size distribution of BCP thin films can be affected by several factors like volume fraction of the individual blocks, polydispersity of the BCP, and homopolymer content in the BCP.[24,57] Although blends of homopolymer and BCP have been widely used to obtain a range of morphologies, it is advantageous to first develop pure BCPs that can be further formulated with known amounts of homopolymer of either blocks to enable the precise control of the thin film morphology.[58–65]

As demonstrated above, the DBU catalyzed BCPs formed low molecular weight side products which we attribute to three possible reasons. First, it has been shown that the ROP of cyclic carbonates can undergo intramolecular transesterification or back-biting reactions resulting in cyclic oligomeric side products.[66] In the case of chain extension of TMC from PS-OH macroinitiator, any backbiting reaction will result in homopolymer of TMC as an impurity. Second, Endo and coworkers have shown that DBU itself can initiate the ROP of six-membered cyclic carbonate monomers to form polymers.[67] This indicates that in addition to the chain extension of the PS-OH macroinitiator to form the diblock copolymer, DBU catalyzed ROP of cyclic carbonate monomers can form homopolymer as a side product. Finally, although all reagents used in this study were anhydrous and great efforts were undertaken to thoroughly dry the PS-OH macroinitiator and TMC monomer, the presence of any residual water in the reaction mixture can also initiate the polymerization of TMC to form PTMC homopolymer impurity via the activated monomer mechanism.[68]

To further verify the assumption that the low molecular weight tail seen in the GPC traces of DBU catalyzed PS-*b*-PTMC BCPs were indeed from PTMC homopolymer, efforts were undertaken to isolate and characterize the impurity. It was observed that while the PTMC homopolymer precipitated in methanol, it was soluble in 60:40 (v/v) methanol:acetonitrile (MeOH:MeCN) solvent mixture. Thus any PTMC homopolymer impurity in the PS-*b*-PTMC BCPs could be removed by fractionating the BCPs in 60:40 (v/v) MeOH:MeCN mixture. While the DPP catalyzed BCP did not show any appreciable change in the molecular weights of the PTMC block by ^{1}H NMR as expected, the DBU catalyzed BCPs showed significantly lower PTMC contents for both the 90 and 50% conversion of TMC monomers after fractionation in MeOH:MeCN mixture. Figure 2 shows ^{1}H NMR plots for the DBU-catalyzed PS-*b*-PTMC BCP stopped at 90% conversion of the TMC monomer before fractionation in MeOH:MeCN (Table 1, Example 1) and the MeOH:MeCN soluble impurity obtained after evaporating the solvent mixture. The NMR plot for the isolated impurity showed majority of the peaks at 4.25 and 2.05 ppm corresponding to PTMC homopolymer (highlighted in blue and green), while the peaks corresponding to the aromatic protons of the polystyrene were minimal (highlighted in yellow).

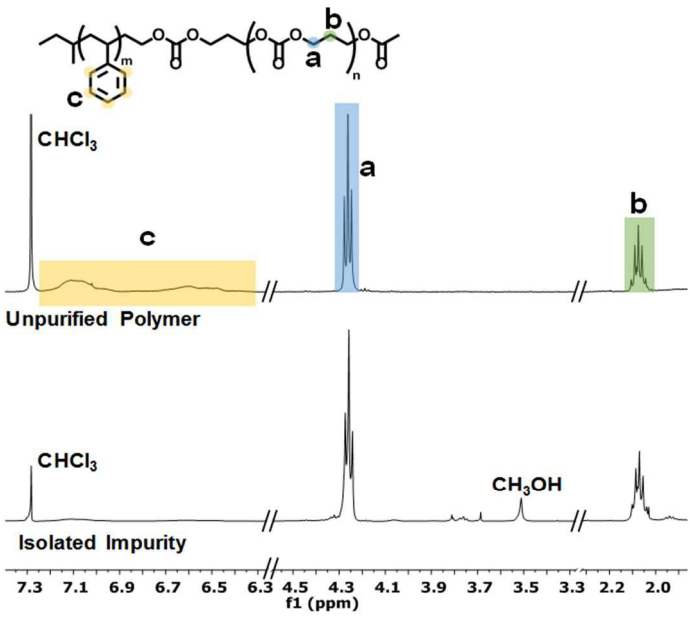

Figure 2. ^{1}H-NMR spectra of DBU catalyzed PS-*b*-PTMC at 90% conversion of TMC monomer before purification (top) and the isolated impurity (bottom) which was identified as primarily PTMC homopolymer. Characteristic signals of PS and PTMC are highlighted in green, blue and yellow.

The GPC trace for the fractionated BCP (Figure 3) showed nearly complete removal of the low molecular weight shoulder and the PDI narrowed from 1.08 to 1.05 (Table 1, Example 1, after fractionation). In contrast, the GPC traces for the DPP-catalyzed BCPs showed minimal change after fractionation in MeOH:MeCN (Figure S3). From these results we conclude that the DBU catalyzed BCP has significant amount of PTMC homopolymer impurity and MeOH:MeCN is an effective solvent mixture to remove the impurity resulting in high quality BCPs which are advantageous for controlled thin film self-assembly.

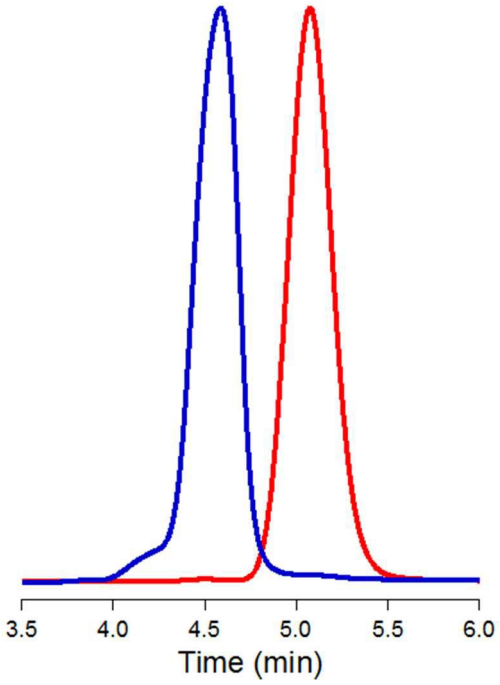

Figure 3. GPC traces for PS-OH (red), M_n = 6600 g/mol, PDI = 1.04 and PS-*b*-PTMC (blue) BCP after precipitating in 60:40 (v/v) MeOH:MeCN solvent mixture. M_n = 14,100 g/mol, PDI = 1.05 (Table 1, Example 1, after fractionation)

Contrast Enhanced Diffusion Ordered Spectroscopy (CEDOSY) of PS-b-PTMC BCPs. Using GPC and ^{1}H NMR analysis for PS-*b*-PTMC BCPs before and after fractionation in MeOH:MeCN, we were able to confirm that PTMC homopolymer impurity is indeed present in the organocatalyzed BCPs obtained after precipitation in MeOH only. While the detection of impurity using conventional methods like GPC and ^{1}H NMR was easy for the DBU catalyzed BCPs due to the large presence of homopolymer content, it can be very challenging to detect very small amounts of homopolymer impurity due to resolution limitations of these techniques. Since homopolymer-free BCPs are desirable for thin film self assembly applications, a quick, reliable and simple method would be valuable to detect small amounts of homopolymer

impurities in the PS-*b*-PTMC BCPs. To this end, the use of NMR technique diffusion ordered spectroscopy (DOSY) that can separate polymeric species according to their size was explored. DOSY offers the potential to investigate mixtures of chemical species in solution where differences in the species hydrodynamic radii (R_h) lead to different rates of diffusion enabling the virtual separation of chemical species according to their R_h and thus size.[69] This powerful technique has been utilized in a variety of systems including polymeric mixtures, small molecules as well as supramolecular complexes[70–73] and is particularly effective when the R_h (and molecular weights) of mixtures are significantly different and there are discrete separated resonances for individual components. However, as the R_h of components become increasingly similar and their resonances overlap it becomes increasingly difficult to resolve mixtures using this technique. There have been a number of elegant examples that have extended the resolution of DOSY of complex mixtures by the addition of a matrix, for instance.[74,75] Beyond sample treatment, there have also been some impactful developments in more sophisticated fitting functions to account for a large number of components in solution.[76–79]

Initially, a DBU catalyzed PS-*b*-PTMC sample known to contain PTMC homopolymer impurity (Table 1, Example 1) was analyzed using DOSY. The decay of the signal intensity of polycarbonate protons **a** vs. gradient strength could be fitted to a single exponential decay and only one diffusion coefficient (D) could be calculated from the fitting parameters according to Stajeskal-Tanner equation (Figure 4).[80] This result suggests that only a single polymeric component was present in solution, contradicting the results obtained by GPC and ^{1}H NMR analysis of this example. In addition, after fractionation in MeOH:MeCN the isolated soluble polymeric fraction was found to be mostly PTMC homopolymer (by ^{1}H NMR). GPC analysis of

this PTMC homopolymer indicated a significantly different molecular weight compared to PS-*b*-PTMC BCP (8k vs. 16k) and therefore a difference in the R_h between these polymers was anticipated which would result in the observation of two distinct diffusion coefficients using DOSY. However, only a single diffusion coefficient was observed by DOSY which, considering the GPC and ^{1}H-NMR data, suggested that homopolymer PTMC and PS-*b*-PTMC adopted a similar R_h in $CDCl_3$ and thus exhibited similar diffusion coefficients. Furthermore, the ability to resolve diffusion coefficients of this mixture was complicated by the signal overlap between the methylene protons of the PTMC homopolymer and those of the PS-*b*-PTMC (Figure 4b).

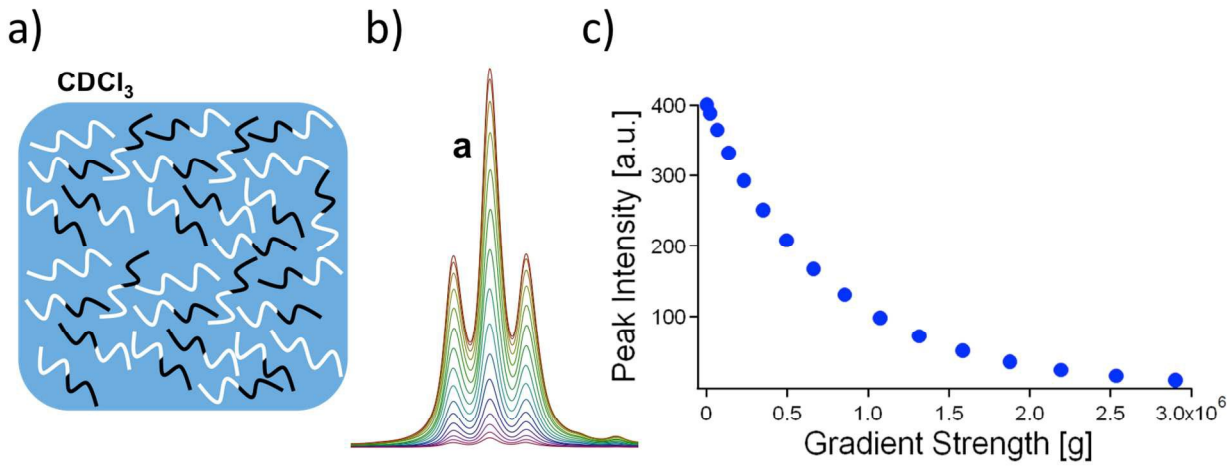

Figure 4. DOSY of PS-*b*-PTMC mixture with homopolymer PTMC: (a) schematic representation of polymeric mixture consisting of BCP (black & white) and PTMC homopolymer (white), (b) plots of PS-*b*-PTMC ^{1}H-NMR increments following polycarbonate proton **a** (peak @ 4.25 ppm) and (c) plot of peak intensity vs. gradient strength

As a simple DOSY experiment was unable to resolve the two polymeric species, a new method to increase the contrast between BCP and homopolymer impurity was developed by forcing the PS-*b*-PTMC BCP component of the mixture to aggregate while maintaining the PTMC homopolymer component of the mixture soluble. This was achieved by using a mixture of two solvents that enabled the formation of stable BCP aggregates (over the duration of experiment) while being a good solvent for the homopolymer impurity, which remained soluble (Figure 5a). The different hydrodynamic radii of aggregated BCP and solvated homopolymer significantly enhances the contrast between their diffusion coefficients. Therefore, we have applied DOSY to this system in a technique we refer to as contrast enhanced DOSY (CEDOSY).

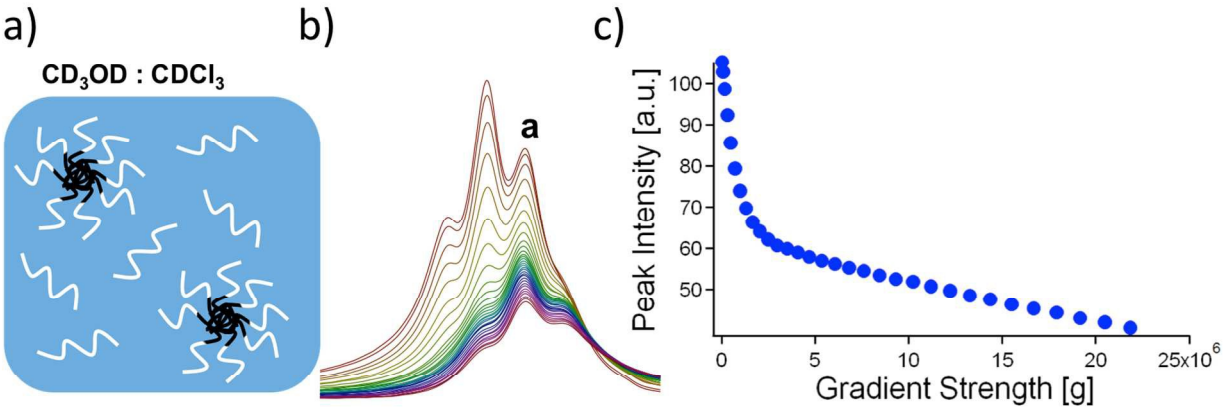

Figure 5. CEDOSY of PS-*b*-PTMC mixture with homopolymer PTCMC in a $CDCl_3/CD_3OD$ solvent: (a) schematic representation of solvent selection to encourage aggregate formation of BCPs while PTMC homopolymer (white) remains soluble, (b) plots of PS-*b*-PTMC ^{1}H-NMR increments following peak polycarbonate proton **a** (peak @ 3.90 ppm) and (c) plot of peak intensity vs. gradient strength.

After screening various solvent mixtures, 55:45 (v/v) CD_3OD:$CDCl_3$ was found to be an ideal solvent blend where the PS-*b*-PTMC BCP formed stable aggregates (cloudy solution) over the course of the CEDOSY experiment time (20-30 minutes) and the PTMC homopolymer remained in solution. A DOSY experiment conducted by dissolving a 8000 g/mol PTMC homopolymer in this solvent mixture showed a single quickly diffusing specie for the clear and unturbid solution. This result confirmed that the homopolymer was indeed soluble in the solvent mixture and did not form aggregates.

In this mixed solvent system the CEDOSY data for the PS-*b*-PTMC BCP before fractionation (Table 1, Example 1) was dramatically different and the decay of the signal of the polycarbonate proton **a** was found to be more complex. Instead of a single exponential decay as described above for the single solvent system ($CDCl_3$), multiple slopes were observed for the mixed solvent system (CD_3OD:$CDCl_3$) for the same BCP sample (Figure 5c). At low gradient strength (ca. 10^5-10^6), a fast decay of the intensity of signal **a** was observed, indicating a quickly diffusing specie, i.e., PTMC homopolymer in this case. The rate of signal decay then dramatically slowed down at higher gradient strengths. This more slowly decaying regime was consistent with the presence of a much larger polymeric material or aggregate in solution, i.e., PS-*b*-PTMC BCP. Control experiments were performed to ensure correct interpretation of the CEDOSY data (see SI). These results showed that using a mixed solvent system, different polymeric components with complete NMR signal overlap and similar R_h values can be resolved by introducing selective aggregation of one of the components.

CEDOSY experiments were also used to qualitatively determine the purity of PS-*b*-PTMC BCP obtained after two precipitations in MeOH and the number of fractionation steps required to

remove the homopolymer PTMC impurity to obtain purified BCPs (Figure 6). For the DBU catalyzed PS-*b*-PTMC BCP (Table 1, Example 1) it was observed that while the signal for the quickly diffusing PTMC homopolymer impurity was significantly reduced, it was still present and a two exponential decays were observed (Figure 6a) after one fractionation step in 60:40 (v/v) MeOH:MeCN solvent mixture. In contrast, the GPC trace for the fractionated BCP (Figure 3) did not show the low molecular tail after the first fraction step, suggesting that only one fractionation step was enough to remove PTMC homopolymer contamination. On the other hand, the CEDOSY experiments still showed the presence of a low molecular weight specie after one fractionation. Two solvent fractionation steps of the BCP were required in order to remove the majority of PTMC homopolymer as detected by CEDOSY. After two fractionation steps, the BCP exhibited a single slow exponential signal decay indicating the presence of only one large aggregated specie in solution and the signal decay for a quickly diffusing species was no longer observed.

This method was also used to examine the effect of organocatalysts (DBU vs. DPP) on polymer purity. The CEDOSY experiments further confirmed the GPC and ^{1}H NMR results that the DBU catalyzed ROP of TMC produced more PTMC homopolymer impurity than the DPP catalyzed reaction. For the DPP catalyzed ROP reaction (Table 1, Example 2), the BCP before fractionation showed two slopes, indicating the presence of PTMC homopolymer and PS-b-PTMC BCP (Figure 6b, blue trace). The signal decay corresponding to the PTMC homopolymer was completely eliminated after only one fractionation step of the BCP in MeOH:MeCN solvent mixture for the DPP catalyzed reaction (Figure 6b, red trace) indicating that majority of the impurity was removed from the BCP. To elucidate the presence of PTMC homopolymer, one should focus not

as much on the peak intensity, but whether the data follows a single or multi-exponential behavior. Therefore, it is important to note that while a systematic change in peak intensity was observed upon fractionations for the DBU catalyzed ROP of TMC, the same trend was not observed when the DPP catalyst was used.

These experiments show that CEDOSY provides a simple and rapid spectroscopic determination of the quality of BCPs as synthesized and the effectiveness of purification conditions to afford clean materials needed for lithographic applications. Ongoing work is focused on determining the limitations of this method and potential to quantify the amount of impurity present in a polymer mixture.

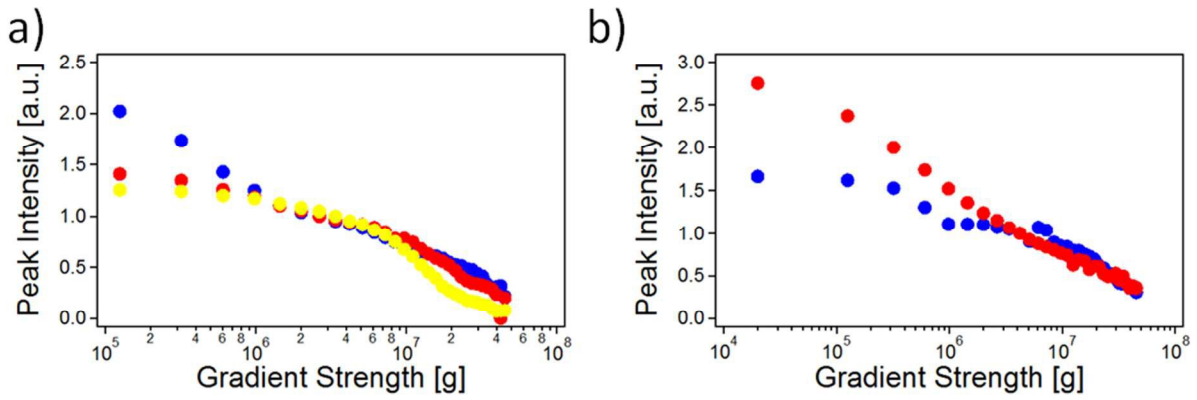

Figure 6. Experimental data from CEDOSY following the decay of methylene protons of signal **a** from isolated impurity, before and after solvent fractionation: (a) plots for PS-*b*-PTMC BCPs catalyzed by DBU to 90% conversion and (b) plots for polymerization catalyzed by DPP at 90% conversion including before (blue), after one fractionation (red) and after two fractionations (yellow).

Thin Film Morphology Study of the Block Copolymers. For lithographic applications, precise control over the morphologies and orientation of the block copolymer thin films is necessary.

Any changes in the BCP composition resulting from reaction conditions and purification steps can significantly impact the thin film uniformity, morphology, and critical dimension (CD) uniformity. Thin film morphology study of PS-*b*-PTMC BCP was undertaken to elucidate the impact of catalyst choice and BCP purification conditions. PGMEA solutions of PS-*b*-PTMC BCPs obtained before and after fractionation in 60:40 (v/v) MeOH:MeCN were spin coated and annealed at 140 °C on PMMA brush grafted silicon wafer coupons. AFM analysis of a 5 µm x 5 µm scan area of the BCP before fractionation, with PTMC Vf_{PTMC} ~ 0.48 (Table 1, Example 1), revealed an island type morphology with a step height of 17 nm (Figure 7a), which is equal to the domain periodicity, Lo, of the BCP. For PS-*b*-PTMC thin films both the BCP-PMMA UL and BCP-air interfaces are preferentially wetted by the PS block of the BCP, forming symmetric wetting layers of PS at the substrate and the air interface resulting in the formation of terrace type features with step heights equal to the pitch of the BCP.[57] GISAXS analysis (Figure 8a) of the same wafer coupon also indicated the presence of parallel lamellae as no higher order peaks in the in-plane scattering direction were observed. The periodicity of the lamellae was calculated from the 1st order Bragg peak to be 18 nm.

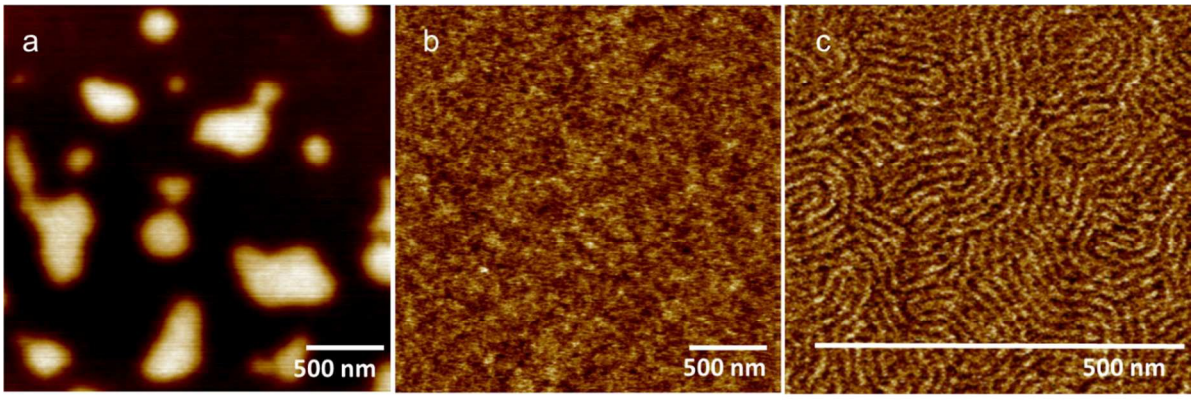

Figure 7. AFM images of PS-*b*-PTMC thin films on PMMA modified substrates: (a) height image of PS-*b*-PTMC BCP before fractionation, Vf_{PTMC} ~ 0.47, (Table 1, Example 1) (b) height image of

the BCP after fractionation, Vf_{PTMC} ~ 0.36 and (c) magnified phase image of BCP after fractionation showing parallel cylinders.

Interestingly, the AFM analysis of the substrate coated with the fractionated PS-*b*-PTMC sample, now with Vf_{PTMC} ~ 0.36 (Table 2, Example 1) showed a smooth film without any terrace type structures (Figure 7b). A 1 µm x 1 µm AFM image (Figure 7c) showed line features corresponding to parallel cylinders of PTMC blocks in PS matrix. In addition, the first order Bragg peak in the GISAXS pattern narrows and shifts to higher scattering vectors, indicating a larger grain size with a smaller periodicity of 16 nm (Figure 8a).

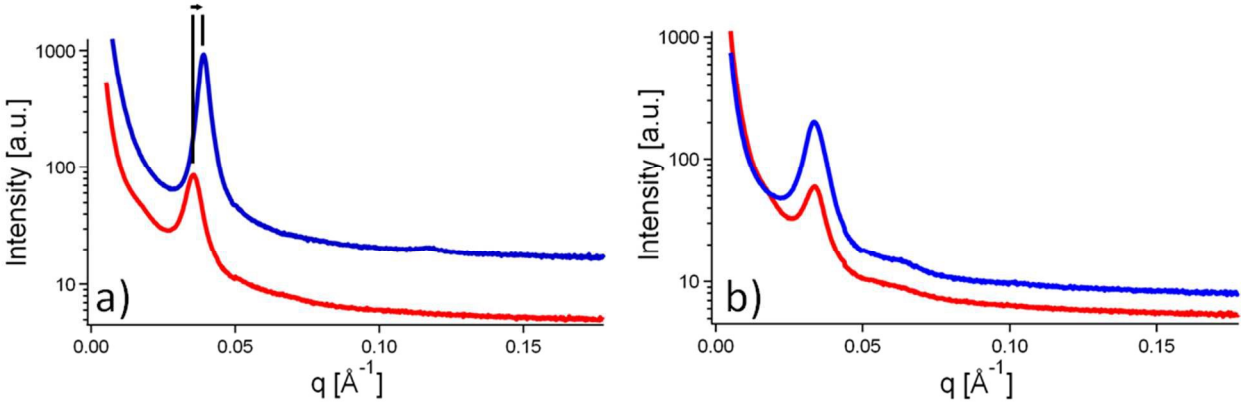

Figure 8. In-plane GISAXS profiles of PS-*b*-PTMC before (red) and after (blue) fractionation: (a) DBU catalyzed BCP (Table 1, Example 1) and (b) DPP catalyzed BCP (Table 1, Example 2). The arrows highlight the first order Bragg peak shift towards higher scattering vectors, *q*.

These results confirm that the PTMC homopolymer impurity in the DBU catalyzed BCP has a dramatic effect on the thin film morphology of PS-*b*-PTMC. The homopolymer swells the PTMC phase causing a phase transition towards the lamellar phase and an increase in the periodicity of the block copolymer. Furthermore, homopolymer blended with BCPs are known to stabilize

morphological defects.[81,82] In contrast to the DBU catalyzed BCPs, the AFM analysis for the thin film morphologies of the DPP catalyzed BCPs before and after purification showed very identical results (results not shown here). This was expected since the fractionation from MeOH:MeCN solvent and CEDOSY experiments revealed limited PTMC homopolymer amount in the MeOH precipitated BCPs. This is corroborated by the GISAXS results (Figure 8b) showing no significant shift in the first order scattering peak.

In conclusion, we have shown the importance for judicious selection of reaction conditions, catalyst choice and purification techniques for making well-defined and clean polycarbonate-containing block copolymers for thin film self-assembly applications. Our results strongly suggested that DPP served as a better catalyst than DBU for making PS-*b*-PTMC BCP with limited PTMC homopolymer impurity and a very small high molecular weight shoulder (< 3%) that did not affect the thin film morphology of the BCP. Control over the periodicity of the block copolymers, as well as domain morphology, orientation, and size uniformity are absolutely crucial for utilizing BCPs in lithographic applications, thus making high quality block copolymers a necessity.

Summary

High quality PS-*b*-PTMC BCPs for thin film self-assembly application were developed using organocatalytic ROP of TMC from a PS-OH macroinitiator. Both base (DBU) and acid (DPP) catalysts were used to study the effect of catalyst choice on the final BCP quality. The GPC trace for the DPP catalyzed BCP showed a very narrow PDI with minimal homopolymer impurity. On the other hand, the DBU catalyzed BCP had a significant homopolymer contamination with a

trimodal GPC trace at higher conversion (~90%) of the TMC monomer. While simple precipitation of the PS-*b*-PTMC in methanol was insufficient to eliminate PTMC homopolymer impurity from the BCP, fractionation in 60:40 (v/v) MeOH:MeCN mixture enabled the removal of the homopolymer resulting in highly clean BCPs. To further analyze the purity of the BCPs before and after purification, a novel contrast enhanced diffusion ordered spectroscopy (CEDOSY) technique was developed. The CEDOSY confirmed that the DBU catalyzed BCP resulted in significant PTMC homopolymer side-products, whereas the DPP catalyzed BCP has minimal homopolymer impurity. Thin film characterization by AFM and GISAXS of the DBU catalyzed BCP showed that the morphology and pitch are changing upon purifying the BCP. With access to clean PS-*b*-PTMC BCP, future work includes balancing the BCP-air and BCP-substrate interfacial energies to enable perpendicular orientation of the BCP and directed self-assembly to align the domains necessary for lithography applications.

ASSOCIATED CONTENT

Supporting Information. Details of CEDOSY data analysis, additional GPC traces, GISAXS and XRR results.

AUTHOR INFORMATION

Corresponding Author

* Email: Ankit Vora <avora@us.ibm.com>

Author Contributions

The manuscript was written through contributions of all authors. All authors have given approval to the final version of the manuscript.

Acknowledgements

The authors would like to acknowledge Krystelle Lionti for measuring the density of PTMC homopolymer. The authors are also thankful to Durairaj Baskaran, Guanyang Lin and Margareata Paunescu from EMD Performance Materials Corporation for providing PS-OH macroinitiator and PMMA brush. Finally, the help of Michael Roders and Alexander Ayzner for measuring GISAXS is appreciated. GISAXS measurements were performed at Beamline 7.3.3 of the Advanced Light Source which is supported by the Director of the Office of Science, Office of Basic Energy Sciences, of the U.S. Department of Energy under Contract No. DE-AC02-05CH11231.

References

1 F. S. Bates and G. H. Fredrickson, *Annu. Rev. Phys. Chem.*, 1990, **41**, 525–557.
2 F. S. Bates and G. H. Fredrickson, *Phys. Today*, 2008, **52**, 32–38.
3 I. W. Hamley and others, *The physics of block copolymers*, Oxford University Press New York, 1998, vol. 19.
4 P. Alexandridis and B. Lindman, *Amphiphilic Block Copolymers: Self-Assembly and Applications*, Elsevier, 2000.
5 H. J. Spinelli, *Adv. Mater.*, 1998, **10**, 1215–1218.
6 S. B. Darling, *Energy Environ. Sci.*, 2009, **2**, 1266.
7 N. Nishiyama, *Nat. Nanotechnol.*, 2007, **2**, 203–204.
8 E. A. Jackson and M. A. Hillmyer, *ACS Nano*, 2010, **4**, 3548–3553.
9 A. Urbas, R. Sharp, Y. Fink, E. L. Thomas, M. Xenidou and L. J. Fetters, *Adv. Mater.*, 2000, **12**, 812–814.
10 H.-C. Kim, S.-M. Park and W. D. Hinsberg, *Chem. Rev.*, 2009, **110**, 146–177.
11 M. Park, C. Harrison, P. M. Chaikin, R. A. Register and D. H. Adamson, *Science*, 1997, **276**, 1401–1404.
12 S. Ouk Kim, H. H. Solak, M. P. Stoykovich, N. J. Ferrier, J. J. de Pablo and P. F. Nealey, *Nature*, 2003, **424**, 411–414.
13 J. Y. Cheng, C. A. Ross, E. L. Thomas, H. I. Smith and G. J. Vancso, *Appl. Phys. Lett.*, 2002, **81**, 3657–3659.
14 C. Tang, E. M. Lennon, G. H. Fredrickson, E. J. Kramer and C. J. Hawker, *Science*, 2008, **322**, 429–432.
15 S.-M. Park, M. P. Stoykovich, R. Ruiz, Y. Zhang, C. T. Black and P. F. Nealey, *Adv. Mater.*, 2007, **19**, 607–611.
16 H. Tsai, J. W. Pitera, H. Miyazoe, S. Bangsaruntip, S. U. Engelmann, C.-C. Liu, J. Y. Cheng, J. J. Bucchignano, D. P. Klaus, E. A. Joseph, D. P. Sanders, M. E. Colburn and M. A. Guillorn, *ACS Nano*, 2014, **8**, 5227–5232.
17 G. S. Doerk, J. Y. Cheng, G. Singh, C. T. Rettner, J. W. Pitera, S. Balakrishnan, N. Arellano and D. P. Sanders, *Nat. Commun.*, 2014, **5**, 5805.

18 H. Yi, X.-Y. Bao, J. Zhang, C. Bencher, L.-W. Chang, X. Chen, R. Tiberio, J. Conway, H. Dai, Y. Chen, S. Mitra and H.-S. P. Wong, *Adv. Mater.*, 2012, **24**, 3107–3114.
19 R. Ruiz, N. Ruiz, Y. Zhang, R. L. Sandstrom and C. T. Black, *Adv. Mater.*, 2007, **19**, 2157–2162.
20 L. Wan, R. Ruiz, H. Gao, K. C. Patel, T. R. Albrecht, J. Yin, J. Kim, Y. Cao and G. Lin, *ACS Nano*, 2015, **9**, 7506–7514.
21 M. D. Rodwogin, C. S. Spanjers, C. Leighton and M. A. Hillmyer, *ACS Nano*, 2010, **4**, 725–732.
22 Y. S. Jung and C. A. Ross, *Nano Lett.*, 2007, **7**, 2046–2050.
23 K. Aissou, M. Mumtaz, G. Fleury, G. Portale, C. Navarro, E. Cloutet, C. Brochon, C. A. Ross and G. Hadziioannou, *Adv. Mater.*, 2015, **27**, 261–265.
24 C. M. Bates, T. Seshimo, M. J. Maher, W. J. Durand, J. D. Cushen, L. M. Dean, G. Blachut, C. J. Ellison and C. G. Willson, *Science*, 2012, **338**, 775–779.
25 T. Hirai, M. Leolukman, T. Hayakawa, M. Kakimoto and P. Gopalan, *Macromolecules*, 2008, **41**, 4558–4560.
26 J. D. Cushen, C. M. Bates, E. L. Rausch, L. M. Dean, S. X. Zhou, C. G. Willson and C. J. Ellison, *Macromolecules*, 2012, **45**, 8722–8728.
27 S. Park, D. H. Lee, J. Xu, B. Kim, S. W. Hong, U. Jeong, T. Xu and T. P. Russell, *Science*, 2009, **323**, 1030–1033.
28 I. Keen, A. Yu, H.-H. Cheng, K. S. Jack, T. M. Nicholson, A. K. Whittaker and I. Blakey, *Langmuir*, 2012, **28**, 15876–15888.
29 T. Hirai, M. Leolukman, C. C. Liu, E. Han, Y. J. Kim, Y. Ishida, T. Hayakawa, M. Kakimoto, P. F. Nealey and P. Gopalan, *Adv. Mater.*, 2009, **21**, 4334–4338.
30 S. Ji, C.-C. Liu, J. G. Son, K. Gotrik, G. S. Craig, P. Gopalan, F. J. Himpsel, K. Char and P. F. Nealey, *Macromolecules*, 2008, **41**, 9098–9103.
31 S. Kim, P. F. Nealey and F. S. Bates, *ACS Macro Lett.*, 2012, **1**, 11–14.
32 J. Cheng, R. A. Lawson, W.-M. Yeh, N. D. Jarnagin, L. M. Tolbert and C. L. Henderson, in *Proc. SPIE*, 2013, vol. 8680, p. 86801V–86801V–4.
33 N. E. Kamber, W. Jeong, R. M. Waymouth, R. C. Pratt, B. G. Lohmeijer and J. L. Hedrick, *Chem. Rev.*, 2007, **107**, 5813–5840.
34 A. P. Dove, *ACS Macro Lett.*, 2012, **1**, 1409–1412.
35 R. P. Brannigan, A. Walder and A. P. Dove, *J. Polym. Sci. Part Polym. Chem.*, 2014, **52**, 2279–2286.
36 K. Fukushima, R. C. Pratt, F. Nederberg, J. P. K. Tan, Y. Y. Yang, R. M. Waymouth and J. L. Hedrick, *Biomacromolecules*, 2008, **9**, 3051–3056.
37 O. Coulembier, S. Moins, S. Maji, Z. Zhang, B. G. De Geest, P. Dubois and R. Hoogenboom, *J. Mater. Chem. B*, 2015, **3**, 612–619.
38 E. A. Appel, V. Y. Lee, T. T. Nguyen, M. McNeil, F. Nederberg, J. L. Hedrick, W. C. Swope, J. E. Rice, R. D. Miller and J. Sly, *Chem. Commun.*, 2012, **48**, 6163–6165.
39 B. Rasmussen and J. B. Christensen, *Org. Biomol. Chem.*, 2012, **10**, 4821–4835.
40 M. K. Kiesewetter, E. J. Shin, J. L. Hedrick and R. M. Waymouth, *Macromolecules*, 2010, **43**, 2093–2107.
41 H. Sardon, A. Pascual, D. Mecerreyes, D. Taton, H. Cramail and J. L. Hedrick, *Macromolecules*, 2015, **48**, 3153–3165.
42 F. Suriano, R. Pratt, J. P. Tan, N. Wiradharma, A. Nelson, Y.-Y. Yang, P. Dubois and J. L. Hedrick, *Biomaterials*, 2010, **31**, 2637–2645.
43 A. L. Lee, S. Venkataraman, S. B. Sirat, S. Gao, J. L. Hedrick and Y. Y. Yang, *Biomaterials*, 2012, **33**, 1921–1928.
44 Y. Li, K. Fukushima, D. J. Coady, A. C. Engler, S. Liu, Y. Huang, J. S. Cho, Y. Guo, L. S. Miller, J. P. Tan and others, *Angew. Chem. Int. Ed.*, 2013, **52**, 674–678.

45 A. Pascual, J. P. Tan, A. Yuen, J. M. Chan, D. J. Coady, D. Mecerreyes, J. L. Hedrick, Y. Y. Yang and H. Sardon, *Biomacromolecules*, 2015, **16**, 1169–1178.
46 P.-C. Zheng, J. Cheng, S. Su, Z. Jin, Y.-H. Wang, S. Yang, L.-H. Jin, B.-A. Song and Y. R. Chi, *Chem.- Eur. J.*, 2015, **21**, 9984–9987.
47 W. Thongsomboon, M. Sherwood, N. Arellano and A. Nelson, *ACS Macro Lett.*, 2012, **2**, 19–22.
48 A. Hexemer, W. Bras, J. Glossinger, E. Schaible, E. Gann, R. Kirian, A. MacDowell, M. Church, B. Rude and H. Padmore, in *Journal of Physics: Conference Series*, IOP Publishing, 2010, vol. 247, p. 012007.
49 J. Ilavsky and P. R. Jemian, *J. Appl. Crystallogr.*, 2009, **42**, 347–353.
50 A. S. Zalusky, R. Olayo-Valles, J. H. Wolf and M. A. Hillmyer, *J. Am. Chem. Soc.*, 2002, **124**, 12761–12773.
51 F. Nederberg, B. G. Lohmeijer, F. Leibfarth, R. C. Pratt, J. Choi, A. P. Dove, R. M. Waymouth and J. L. Hedrick, *Biomacromolecules*, 2007, **8**, 153–160.
52 D. J. Coady, H. W. Horn, G. O. Jones, H. Sardon, A. C. Engler, R. M. Waymouth, J. E. Rice, Y. Y. Yang and J. L. Hedrick, *ACS Macro Lett.*, 2013, **2**, 306–312.
53 K. Makiguchi, Y. Ogasawara, S. Kikuchi, T. Satoh and T. Kakuchi, *Macromolecules*, 2013, **46**, 1772–1782.
54 S. Tempelaar, L. Mespouille, P. Dubois and A. P. Dove, *Macromolecules*, 2011, **44**, 2084–2091.
55 Y. E. Aguirre-Chagala, J. L. Santos, R. Herrera-Nájera and M. Herrera-Alonso, *Macromolecules*, 2013, **46**, 5871–5881.
56 R. C. Pratt, B. G. Lohmeijer, D. A. Long, R. M. Waymouth and J. L. Hedrick, *J. Am. Chem. Soc.*, 2006, **128**, 4556–4557.
57 S. Kim, C. M. Bates, A. Thio, J. D. Cushen, C. J. Ellison, C. G. Willson and F. S. Bates, *ACS Nano*, 2013, **7**, 9905–9919.
58 D. J. Kinning, K. I. Winey and E. L. Thomas, *Macromolecules*, 1988, **21**, 3502–3506.
59 H. Tanaka, H. Hasegawa and T. Hashimoto, *Macromolecules*, 1991, **24**, 240–251.
60 T. Hashimoto, H. Tanaka and H. Hasegawa, *Macromolecules*, 1990, **23**, 4378–4386.
61 K. I. Winey, E. L. Thomas and L. J. Fetters, *Macromolecules*, 1991, **24**, 6182–6188.
62 A. M. Mayes, T. P. Russell, S. K. Satija and C. F. Majkrzak, *Macromolecules*, 1992, **25**, 6523–6531.
63 U. Jeong, D. Y. Ryu, D. H. Kho, D. H. Lee, J. K. Kim and T. P. Russell, *Macromolecules*, 2003, **36**, 3626–3634.
64 G. Liu, M. P. Stoykovich, S. Ji, K. O. Stuen, G. S. W. Craig and P. F. Nealey, *Macromolecules*, 2009, **42**, 3063–3072.
65 A. Vora, B. Zhao, D. To, J. Y. Cheng and A. Nelson, *Macromolecules*, 2010, **43**, 1199–1202.
66 H. Keul in *Handbook for Ring-Opening Polymerization,* ed. P. Dubois, O. Coulembier, J-M. Raquez, Wiley-VCH Verlag GmbH & Co. KGaA, Weinheim, 2009, 12, 307.
67 T. Endo, K. Kakimoto, B. Ochiai and D. Nagai, *Macromolecules*, 2005, **38**, 8177–8182.
68 D. Delcroix, B. Martín-Vaca, D. Bourissou and C. Navarro, *Macromolecules*, 2010, **43**, 8828–8835.
69 K. F. Morris, P. Stilbs and C. S. Johnson, *Anal. Chem.*, 1994, **66**, 211–215.
70 A. Jerschow and N. Müller, *Macromolecules*, 1998, **31**, 6573–6578.
71 D. A. Jayawickrama, C. K. Larive, E. F. McCord and D. C. Roe, *Magn. Reson. Chem.*, 1998, **36**, 755–760.
72 Y. Cohen, L. Avram and L. Frish, *Angew. Chem. Int. Ed.*, 2005, **44**, 520–554.
73 R. J. Wojtecki, Q. Wu, J. C. Johnson, D. G. Ray, L. T. J. Korley and S. J. Rowan, *Chem. Sci.*, 2013, **4**, 4440–4448.
74 R. W. Adams, J. A. Aguilar, J. Cassani, G. A. Morris and M. Nilsson, *Org. Biomol. Chem.*, 2011, **9**, 7062–7064.
75 C. F. Tormena, R. Evans, S. Haiber, M. Nilsson and G. A. Morris, *Magn. Reson. Chem. MRC*, 2010, **48**, 550–553.
76 A. A. Colbourne, G. A. Morris and M. Nilsson, *J. Am. Chem. Soc.*, 2011, **133**, 7640–7643.

77 B. R. Martini, V. A. Mandelshtam, G. A. Morris, A. A. Colbourne and M. Nilsson, *J. Magn. Reson. San Diego Calif 1997*, 2013, **234**, 125–134.
78 I. Toumi, B. Torrésani and S. Caldarelli, *Anal. Chem.*, 2013, **85**, 11344–11351.
79 I. Toumi, S. Caldarelli and B. Torrésani, *Prog. Nucl. Magn. Reson. Spectrosc.*, 2014, **81**, 37–64.
80 M. Nilsson, *J. Magn. Reson. San Diego Calif 1997*, 2009, **200**, 296–302.
81 E. Burgaz and S. P. Gido, *Macromolecules*, 2000, **33**, 8739–8745.
82 D. Duque, K. Katsov and M. Schick, *J. Chem. Phys.*, 2002, **117**, 10315–10320.

TOC Figure